arXiv:1611.05236v1 [cond-mat.mes-hall] 16 Nov 2016

Anisotropic magnetotransport in Dirac-Weyl magnetic junctions

Yuya Ominato, Koji Kobayashi, and Kentaro Nomura
Institute for Materials Research, Tohoku University, Sendai 980-8577, Japan
(Dated: November 17, 2016)

We theoretically study the anisotropic magnetotransport in Dirac-Weyl magnetic junctions where a doped ferromagnetic Weyl semimetal is sandwiched between doped Dirac semimetals. We calculate the conductance using the Landauer formula and find that the system exhibits extraordinarily large anisotropic magnetoresistance (AMR). The AMR depends on the ratio of the Fermi energy and the strength of the exchange interaction. The origin of the AMR is the shift of the Fermi surface in the Weyl semimetal and the mechanism is completely different from the conventional AMR originating from the spin dependent scattering and the spin-orbit interaction.

I. INTRODUCTION

Magnetoresistance effects in ferromagnetic materials have been investigated during the past decades for applications to spintronics devices. Several kinds of magnetoresistance effects have been found. Anisotropic magnetoresistance (AMR) is a phenomenon where the resistance depends on the relative angle between the magnetization and the electric current [1]. Typically the angle dependent resistivity/conductivity is of the order of a few percent. Giant magnetoresistance (GMR) is another phenomenon observed in thin-film structures composed of alternating ferromagnetic and non-magnetic conductive layers [2, 3]. In the GMR, the magnetoresistance exhibits several dozen percent, which significantly exceeds the AMR. Searching for stronger magnetoresistance effects such as the tunneling magnetoresistance [4] is a central issue in the field of spintronics.

Recently, magnetotransport in topological materials, such as topological insulators [5, 6] and Dirac/Weyl semimetals [7–11], have drawn much interest for achieving novel electromagnetic coupling via the strong spin-orbit interaction [12–14]. A Dirac semimetal manifests the pseudo-relativistic linear dispersions doubly degenerate with time-reversal and spatial-inversion symmetries, and it is non-magnetic [15–17]. A Weyl semimetal possesses the gapless linear dispersions with broken time-reversal [18–20] or spatial-inversion symmetries [21–27]. In a magnetic Weyl semimetal, time reversal symmetry is broken because of a magnetic ordering. One of the signatures of Dirac/Weyl semimetals is the longitudinal negative magnetoresistance [28–34] that has been observed experimentally in non-magnetic systems [35–44]. The negative magnetoresistance can be observed in both time-reversal and spatial-inversion symmetry broken Weyl semimetals. Here, we study magnetoresistance effects that is peculiar to the time-reversal symmetry broken Weyl semimetals, i.e., magnetic Weyl semimetals.

In this paper, we study the anisotropic magnetotransport in Dirac-Weyl magnetic junctions. We consider a system that consists of a doped ferromagnetic Weyl semimetal sandwiched by doped Dirac semimetals, and calculate the transmission probability through the Dirac-Weyl magnetic junctions. In our system, the Dirac/Weyl semimetals are characterized by the absence/presence of the spontaneous magnetization, which splits the band touching points in momentum space. Using the Landauer formula, we compute the conductance as a function of the relative angle between the magnetization and the electric current. We find that the AMR can be extraordinarily large compared with that of conventional ferromagnetic metals and the AMR has the same periodicity of the conventional AMR as a function of the relative angle. In the Dirac-Weyl magnetic junctions, the mechanism of the AMR is entirely different from the conventional one, which is generally considered to arise from spin dependent scattering and spin-orbit coupling. The shift of the Fermi surface caused by the magnetization in the Weyl semimetal is the origin of the AMR.

The paper is organized as follows. In Sec. II, we introduce a continuous model which describes a Dirac semimetal and a ferromagnetic Weyl semimetal with a pair of Weyl nodes. In Sec. III, we calculate the transmission probability of the Dirac-Weyl magnetic junctions. In Sec. IV, we compute the conductance using the Landauer formula. The conclusion and discussion are given in Sec. V.

II. MODEL HAMILTONIAN

We consider magnetic junctions composed of Dirac and ferromagnetic Weyl semimetals as illustrated in Fig. 1(a), where the doped magnetic Weyl semimetal in region Ⅱ ($0 \le x \le L$) is sandwiched between the doped Dirac semimetals in region Ⅰ and Ⅲ ($x < 0, L < x$). We assume that the Dirac semimetals are semi-infinite in x direction and the system is periodic in y and z direction. The magnetic junction is implemented in the magnetization,

$$\boldsymbol{M}(x) = \begin{cases} (0,0,0) & (x<0, L<x), \\ M_0(\cos\theta, 0, \sin\theta) & (0 \le x \le L), \end{cases} \tag{1}$$

as shown in Fig. 1(a).

We start with a model Hamiltonian for electrons in Dirac/Weyl semimetals,

$$H_0 = \hbar v \tau_z \boldsymbol{\sigma} \cdot (-i\boldsymbol{\nabla}) + \tau_0 J \boldsymbol{M}(x) \cdot \boldsymbol{\sigma}, \tag{2}$$

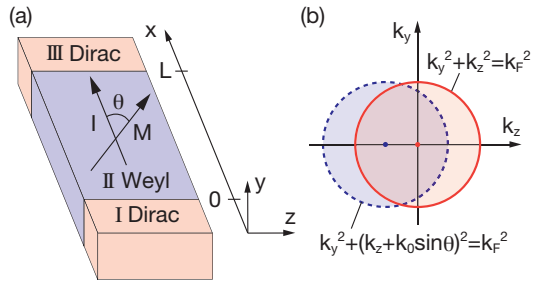

FIG. 1: (a) Dirac-Weyl magnetic junctions composed of Dirac and ferromagnetic Weyl semimetals. The magnetization vector is on the x-z plane and the angle between the magnetization and the x axis is θ. (b) Fermi surfaces of Dirac and Weyl semimetals with positive chirality projected on k_y-k_z plane. The area inside the red solid (blue dashed) circle represents the Fermi surface of the Dirac (Weyl) semimetal.

where v is the velocity, $\boldsymbol{\sigma}$ and $\boldsymbol{\tau}$ are the triplets of Pauli matrices acting on the real spin and the pseudospin (chirality) degrees of freedom, and J is the exchange coupling constant. There are two nodes with positive and negative chirality characterizing the correlation between the spin and the momentum. In region I and Ⅲ (doped Dirac semimetal), there is no magnetic moment, and the energy bands are doubly degenerate. In region Ⅱ (doped Weyl semimetal), the exchange interaction splits the twofold Fermi surfaces in the direction of the magnetization in momentum space. In the present work, we treat two Fermi surfaces with positive and negative chiralities independently, assuming the absence of inter-node scattering. Figure 1(b) shows the Fermi surfaces of the Dirac and Weyl semimetals with positive chirality, projected on k_y-k_z plane. In the presence of the magnetization (in region Ⅱ), the Fermi surface is shifted along the k_z axis by $k_0 \sin\theta$, where

$$k_0 = \frac{JM_0}{\hbar v}. \tag{3}$$

When $k_{\rm F} > k_0 \sin\theta$, where $k_{\rm F}$ is the Fermi wave number, the projected Fermi surfaces of the Dirac and Weyl semimetals are partially overlapped, while not when $k_{\rm F} < k_0 \sin\theta$.

III. TRANSMISSION PROBABILITY

In this section, we calculate transmission probability along x axis for eigenstates of the positive chirality. Due to the translational invariance along y and z axis, the wave numbers k_y and k_z are conserved and an eigenstate is labeled by the wave numbers k_y and k_z in the projected Fermi surface of the Dirac semimetals, $k_y^2 + k_z^2 < k_{\rm F}^2$. The common factor $e^{i(k_y y + k_z z)}$ is omitted in the following expressions.

The wave function can be written in terms of incident and reflected waves. In region I, the two-component wave function is written as

$$\psi_{\rm I}(x) = \begin{pmatrix} k_x - ik_y \\ k_{\rm F} - k_z \end{pmatrix} e^{ik_x x} + r \begin{pmatrix} -k_x - ik_y \\ k_{\rm F} - k_z \end{pmatrix} e^{-ik_x x}, \tag{4}$$

where

$$k_x = \sqrt{k_{\rm F}^2 - k_y^2 - k_z^2}\,. \tag{5}$$

In region Ⅱ, we have

$$\psi_{\rm II}(x) = a \begin{pmatrix} k'_x - ik_y \\ k_{\rm F} - (k_z + k_0 \sin\theta) \end{pmatrix} e^{i(k'_x - k_0\cos\theta)x} + b \begin{pmatrix} -k'_x - ik_y \\ k_{\rm F} - (k_z + k_0 \sin\theta) \end{pmatrix} e^{i(-k'_x - k_0\cos\theta)x}, \tag{6}$$

where

$$k'_x = \sqrt{k_{\rm F}^2 - k_y^2 - (k_z + k_0 \sin\theta)^2}\,. \tag{7}$$

In the case of $k_{\rm F}^2 - k_y^2 - (k_z + k_0 \sin\theta)^2 < 0$, k'_x becomes pure imaginary number, and the wave function describes an evanescent mode decaying exponentially. In region Ⅲ, we have

$$\psi_{\rm III}(x) = t \begin{pmatrix} k_x - ik_y \\ k_{\rm F} - k_z \end{pmatrix} e^{ik_x x}. \tag{8}$$

The continuity of the wave functions at the junctions gives boundary conditions, $\psi_{\rm I}(0) = \psi_{\rm II}(0)$ and $\psi_{\rm II}(L) = \psi_{\rm III}(L)$, and determines the coefficients r, a, b, and t. The transmission probability along x axis is obtained from $T(k_y, k_z, \theta) = |t|^2$ and has the form

$$T(k_y, k_z, \theta) = \frac{4k_x^2 k_x'^2}{4k_x^2 k_x'^2 \cos^2(k'_x L) + \left(k_x^2 + k_x'^2 + k_0^2 \sin^2\theta\right)^2 \sin^2(k'_x L)}. \tag{9}$$

Note that k_x and k'_x are functions of k_y and k_z as given in Eqs. (5) and (7). From the above expression, we see that the transmission probability depends on the z component of the magnetization, giving the shift of the projected Fermi surface, while the x component does not contribute. Therefore, the transmission probability is unity at $\theta = m\pi$ with an integer m.

As shown in Fig. 1(b), the projected Fermi surface of the Dirac semimetals ($k_y^2 + k_z^2 < k_{\rm F}^2$) can be divided into two regions: overlapping region $[k_y^2 + (k_z + k_0 \sin\theta)^2 < k_{\rm F}^2]$, where that of the Weyl semimetal is overlapping, and non-overlapping region $[k_y^2 + (k_z + k_0 \sin\theta)^2 > k_{\rm F}^2]$, where the traveling mode corresponding to the incident wave is absent in the Weyl semimetal. The expression Eq. (9) is applicable also to a pure imaginary k'_x, i.e., the wave function in region Ⅱ is an evanescent mode. The transmission probability behaves in a significantly

different manner in the overlapping (with real k'_x) and non-overlapping (with pure imaginary k'_x) regions.

In the overlapping region, the incident wave is transmitted via the traveling mode in region Ⅱ. From Eq. (9), we can show that the incident wave is transmitted with the transmission probability $T(k_y, k_z, \theta) = 1$ for values of $k'_x L$ satisfying the relation $k'_x L = n\pi$ [45–49], with n a positive integer, corresponding to a condition that a standing wave can exist in the region Ⅱ. The relation is written as

$$k_y^2 + (k_z + k_0 \sin\theta)^2 = k_{\rm F}^2 \left[1 - \left(\frac{n\pi}{k_{\rm F} L}\right)^2\right]. \qquad (10)$$

Figure 2 shows the transmission probability as a function of k_y and k_z at several L's. We set $k_0 = 0.5k_{\rm F}$ and $\theta = \pi/2$ as a typical example. For $k_{\rm F}L < \pi$, there is no solution of Eq. (10), so that there is no peak structure in Fig. 2(a) and the transmission probability satisfies $T(k_y, k_z, \theta) < 1$. In Figs. 2(b), (c), and (d), there are peak structures where the transmission probability is unity on the circles represented by Eq. (10). The number of peaks increases with the increase of $k_{\rm F}L$.

In the non-overlapping region, an evanescent mode in region Ⅱ, $k'_x = i\kappa$ with $\kappa = \sqrt{-k_{\rm F}^2 + k_y^2 + (k_z + k_0 \sin\theta)^2}$, transmits an incident wave and the transmission probability is written as

$$T(k_y, k_z, \theta) = \frac{4k_x^2\kappa^2}{4k_x^2\kappa^2 \cosh^2(\kappa L) + \left(k_x^2 - \kappa^2 + k_0^2 \sin^2\theta\right)^2 \sinh^2(\kappa L)}. \qquad (11)$$

From the above expression, we immediately see that the transmission probability monotonically decreases with the increase of L in an exponential manner. Figure 2 shows that the transmission probability becomes exponentially small.

Figure 3 shows the transmission probability at several k_0's, where we set $k_{\rm F}L = 2$ and $\theta = \pi/2$. For a large k_0, the transmission probability is significantly suppressed even in the overlapping region; the spin-momentum locking causes the discrepancy of the spinors between the incident and traveling modes.

IV. CONDUCTANCE

To characterize the total transmission for the given magnetization direction and magnitude, we calculate the Landauer conductance

$$G(\theta) = 2\frac{e^2}{h} \sum_{k_y k_z} T(k_y, k_z, \theta) = 2\frac{e^2}{h} \frac{S}{(2\pi)^2} \int_D T(k_y, k_z, \theta) dk_y dk_z, \qquad (12)$$

where S is the area of the junctions, and the region D is the projected Fermi surface of the Dirac semimetals,

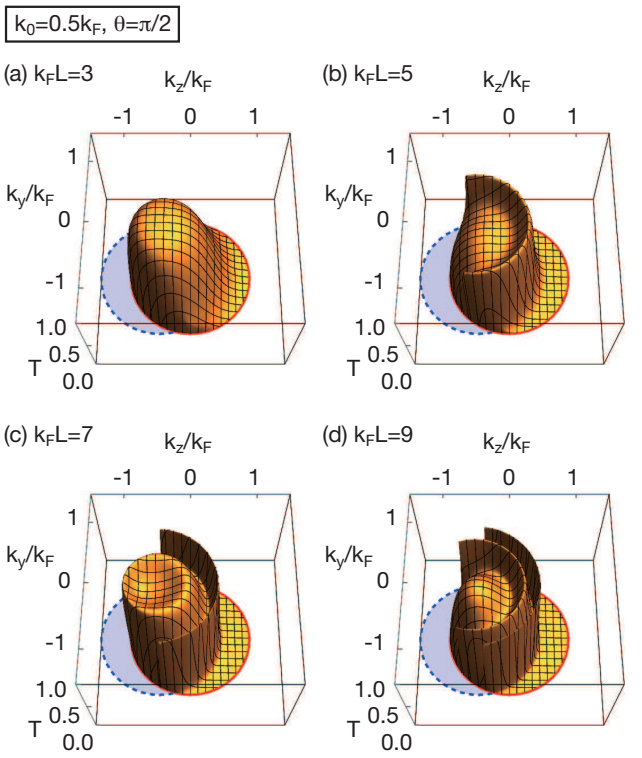

FIG. 2: Transmission probability as a function of k_y and k_z in the Fermi surface of the Dirac semimetals projected on the k_y-k_z plane. Transmission probability is plotted at (a) $k_{\rm F}L = 3$, (b) $k_{\rm F}L = 5$, (c) $k_{\rm F}L = 7$, (d) $k_{\rm F}L = 9$. We set $k_0 = 0.5k_{\rm F}$ and $\theta = \pi/2$.

$k_y^2 + k_z^2 < k_{\rm F}^2$. The factor two comes from the two nodes with positive and negative chiralities giving the same contribution. The conductance $G(\theta)$ is naturally proportional to S, and the conductance per unit area, $G(\theta)/S$, can be used as a quantity that measures the transparency of the magnetic junctions for the electronic transport.

In Fig. 4(a), we plot the conductance, Eq. (12), as a function of θ. Here, we set $k_{\rm F}L = 2$ and $k_0 = 0.5k_{\rm F}$, $k_{\rm F}$, $2k_{\rm F}$. The conductance has a property, $G(\theta + \pi) = G(\theta)$, i.e., $G(\theta)$ has a periodicity of π, which can be derived from Eq. (9), the expression for $T(k_y, k_z, \theta)$, and appropriately changing the integral variable in Eq. (12). At the angles $\theta = m\pi$ with an integer m, the conductance is independent of k_0 and θ, because the transmission probability is unity for the arbitrary incident wave as we mentioned in the previous section. The conductance decreases when the angle θ deviates from $\theta = m\pi$ and reaches a minimum value at $\theta = (m + 1/2)\pi$. This is because the conductance is governed by the area of the overlapping region, and the overlapping area depends only on the shift of the projected Fermi surface $|k_0 \sin\theta|$. Therefore, the conductance decreases with the increase of k_0, as we can see it in Fig. 4(a). At $k_0 = 2k_{\rm F}$, there is no overlapping region at $\theta = (m + 1/2)\pi$, so that the conductance becomes exponentially small.

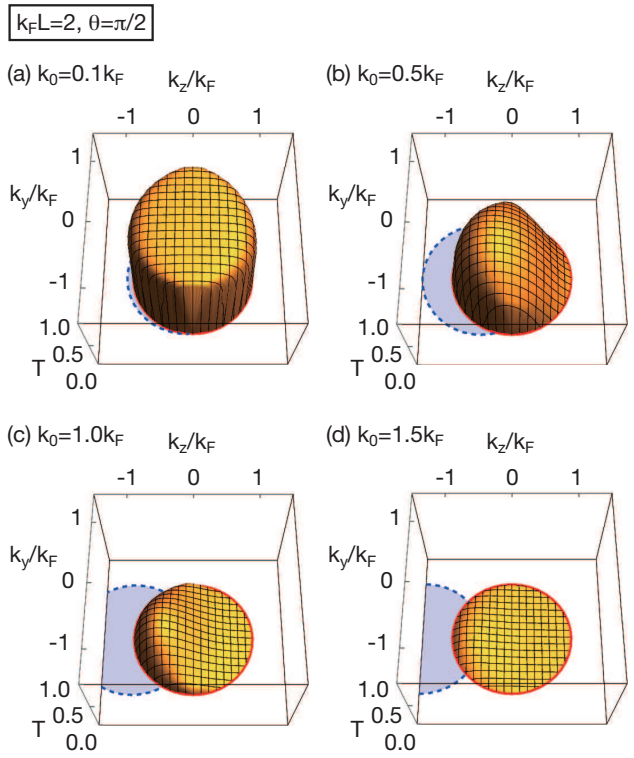

FIG. 3: Transmission probability as a function of k_y and k_z in the Fermi surface of the Dirac semimetals projected on the k_y-k_z plane. Transmission probability is plotted at (a) $k_0 = 0.1k_F$, (b) $k_0 = 0.5k_F$, (c) $k_0 = 1.0k_F$, (d) $k_0 = 1.5k_F$. We set $k_FL = 2$ and $\theta = \pi/2$.

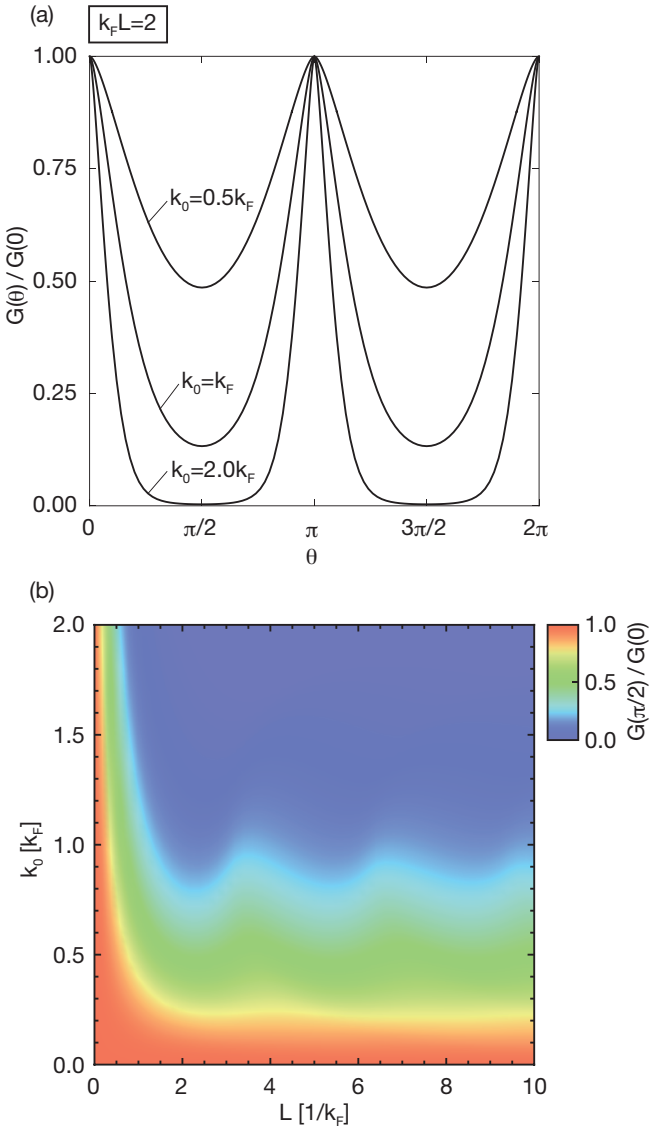

FIG. 4: (a) The conductance $G(\theta)$ as a function of θ. We set $k_FL = 2$ and plot the conductance for $k_0 = 0.5k_F, k_F, 2.0k_F$. (b) The color plot of the ratio of the conductance $G(\pi/2)/G(0)$ as a function of L and k_0.

In Fig. 4(b), the conductance $G(\pi/2)$, which is the minimum value of $G(\theta)$, is plotted as a function of L and k_0. When k_0 is fixed, the conductance decreases with the increase of L because the transmission probability in the non-overlapping region decreases exponentially, and approaches to a minimum value, which is approximately proportional to the area of the overlapping region. Around $k_0 \approx 0.7k_F$, we see oscillatory behavior coming from the peak structures of the transmission probability. The conductance at fixed L decreases with the increase of k_0 because of the decrease of the overlapping area.

V. CONCLUSION AND DISCUSSION

We studied the anisotropic magnetotransport in the Dirac-Weyl magnetic junctions and found that the present system exhibits the extraordinarily large AMR. For the magnetization parallel to the electric current ($\theta = 0$), the conductance is not influenced by the magnetization, while for the magnetization perpendicular to the electric current ($\theta = \pi/2$), the conductance becomes exponentially small for a sufficiently strong exchange interaction and magnetization, i.e., $k_0 \gg k_F$.

Here we discuss the case when the sizes of the Fermi surface in the Dirac and Weyl semimetals are different, and show that the difference does't change the qualitative results. In this paper, we have assumed that the sizes of the Fermi surface are the same, although they can be different in general. In this case, the Hamiltonian is given as

$$H = H_0 + V(x), \tag{13}$$

where $V(x)$ is a potential, shifting the Fermi energy of the Weyl semimetal,

$$V(x) = \begin{cases} 0 & (x < 0, L < x), \\ V_0 & (0 \le x \le L). \end{cases} \tag{14}$$

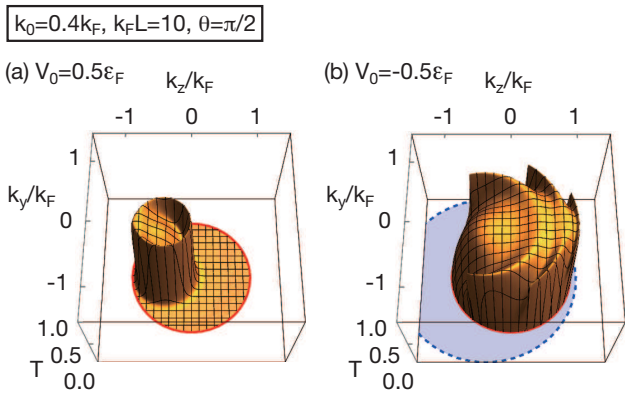

FIG. 5: Transmission probability as a function of k_y and k_z in the Fermi surface of the Dirac semimetals projected on the k_y-k_z plane. Transmission probability is plotted at (a) $V_0 = 0.5\varepsilon_{\rm F}$ and (b) $V_0 = -0.5\varepsilon_{\rm F}$, where $\varepsilon_{\rm F} = \hbar v k_{\rm F}$. We set $k_0 = 0.4k_{\rm F}$, $k_{\rm F}L = 10$, and $\theta = \pi/2$.

In a similar manner to Eq. (9), we derive the transmission probability,

$$T(k_y, k_z, \theta) = \frac{4k_x^2 k_x'^2}{4k_x^2 k_x'^2 \cos^2(k_x' L) + \left[k_x^2 + k_x'^2 + k_0^2 \sin^2\theta - V_0^2/(\hbar v)^2\right]^2 \sin^2(k_x' L)}, \quad (15)$$

where

$$k_x' = \sqrt{\left[k_{\rm F} - V_0/(\hbar v)\right]^2 - k_y^2 - (k_z + k_0 \sin\theta)^2}\ . \quad (16)$$

In Fig. 5, the transmission probability is plotted at (a) $V_0 = 0.5\varepsilon_{\rm F}$ and (b) $V_0 = -0.5\varepsilon_{\rm F}$, where $\varepsilon_{\rm F} = \hbar v k_{\rm F}$. We again observe the peak structures on $k_x' L = n\pi$ and the suppression of the transmission probability originating from the spin-momentum locking.

The origin of the AMR in the present system is the shift of the Fermi surface in the momentum space, which is completely different from that of the conventional AMR in ferromagnetic metal, but we can get an expression for the conductance that resembles the conventional AMR. On condition that $|k_0 \sin\theta|$ is much smaller than the Fermi wave number $k_{\rm F}$, the transmission probability Eq. (9) is approximated by

$$T(k_y, k_z, \theta) \simeq 1 - T_1(k_y, k_z)\left(\frac{k_0 \sin\theta}{k_{\rm F}}\right) - T_2(k_y, k_z)\left(\frac{k_0 \sin\theta}{k_{\rm F}}\right)^2, \quad (17)$$

where we neglect higher order terms than $(k_0 \sin\theta/k_{\rm F})^2$. Substituting Eq. (17) for Eq. (12), we get an approximate expression. The conductance $G(\theta)$ is an even function of θ, i.e., $G(\theta) = G(-\theta)$, because the system with the relative angle $-\theta$ can be transformed into the relative angle θ by rotating the system around x axis. Therefore, the conductance is written as

$$G(\theta) \simeq G(0) - \Delta G \sin^2\theta, \quad (18)$$

where

$$G(0) = 2\frac{e^2}{h}\frac{S}{(2\pi)^2}\pi k_{\rm F}^2,$$
$$\Delta G = 2\frac{e^2}{h}\frac{S}{(2\pi)^2}\int_D T_2(k_y, k_z)\left(\frac{k_0}{k_{\rm F}}\right)^2 dk_y dk_z. \quad (19)$$

The above expression for $G(\theta)$ is similar to the AMR in the conventional ferromagnetic metals [1].

Finally, we mention how to observe the extraordinarily large AMR experimentally. There is a great deal of theoretical and experimental work on searching for magnetic Weyl semimetals. One of the candidate materials is Cr-doped $Bi_2(Se_xTe_{1-x})_3$ [50–52]. The bulk band gap of Bi_2Se_3 can be tuned by substituting tellurium for selenium, and the gap almost closes at the Γ point with the selenium concentration $x \simeq 0.6$ [53, 54]. In the presence of magnetic dopants Cr, we expect the ferromagnetic ordering below a critical temperature and emergence of the Weyl semimetal phase. Therefore, the AMR discussed in the present work can be observed in multilayer structure of non-magnetic and magnetic $Bi_2(Se_xTe_{1-x})_3$. The condition to observe the large AMR is written as $k_{\rm F} \ll k_0$ and $L \gg 1/k_{\rm F}$. Using the parameters for the above material ($JM_0 = 2.0x_iS$[eV], $\hbar v = 2.2$[eVÅ]) [50, 51, 55–57], where x_i is the ratio of the magnetic dopants and $S = 3/2$, we can quantitatively estimate the shift of the Fermi surface k_0. At $x_i = 0.1$, the condition is satisfied when $k_{\rm F} \ll 0.14$[Å^{-1}]($\varepsilon_{\rm F} \ll 0.31$[eV]). In this situation, we can set $k_{\rm F} = 0.01$[Å^{-1}] as a typical value, so that the condition for the system size is written as $L \gg 100$[Å].

ACKNOWLEDGEMENTS

This work was supported by JSPS KAKENHI Grant Numbers JP26400308, JP15H05854, and JP16J01981.

[1] T. McGuire and R. Potter, IEEE Transactions on Magnetics **11**, 1018 (1975).

[2] M. N. Baibich, J. M. Broto, A. Fert, F. N. Van Dau,

F. Petroff, P. Etienne, G. Creuzet, A. Friederich, and J. Chazelas, Physical review letters **61**, 2472 (1988).
[3] G. Binasch, P. Grünberg, F. Saurenbach, and W. Zinn, Physical review B **39**, 4828 (1989).
[4] I. Žutić, J. Fabian, and S. D. Sarma, Reviews of modern physics **76**, 323 (2004).
[5] M. Z. Hasan and C. L. Kane, Reviews of Modern Physics **82**, 3045 (2010).
[6] X.-L. Qi and S.-C. Zhang, Reviews of Modern Physics **83**, 1057 (2011).
[7] S. M. Young, S. Zaheer, J. C. Teo, C. L. Kane, E. J. Mele, and A. M. Rappe, Physical review letters **108**, 140405 (2012).
[8] Z. Wang, Y. Sun, X.-Q. Chen, C. Franchini, G. Xu, H. Weng, X. Dai, and Z. Fang, Physical Review B **85**, 195320 (2012).
[9] S. Murakami, New Journal of Physics **9**, 356 (2007).
[10] X. Wan, A. M. Turner, A. Vishwanath, and S. Y. Savrasov, Physical Review B **83**, 205101 (2011).
[11] A. Burkov and L. Balents, Physical review letters **107**, 127205 (2011).
[12] T. Yokoyama, Y. Tanaka, and N. Nagaosa, Physical Review B **81**, 121401 (2010).
[13] I. Matsuzaki and K. Nomura, arXiv preprint arXiv:1503.04953 (2015).
[14] B. Scharf, A. Matos-Abiague, J. E. Han, E. M. Hankiewicz, and I. Žutić, Phys. Rev. Lett. **117**, 166806 (2016).
[15] Z. Liu, B. Zhou, Y. Zhang, Z. Wang, H. Weng, D. Prabhakaran, S.-K. Mo, Z. Shen, Z. Fang, X. Dai, et al., Science **343**, 864 (2014).
[16] M. Neupane, S.-Y. Xu, R. Sankar, N. Alidoust, G. Bian, C. Liu, I. Belopolski, T.-R. Chang, H.-T. Jeng, H. Lin, et al., Nature communications **5** (2014).
[17] S. Borisenko, Q. Gibson, D. Evtushinsky, V. Zabolotnyy, B. Büchner, and R. J. Cava, Physical review letters **113**, 027603 (2014).
[18] J. Liu, J. Hu, D. Graf, S. Radmanesh, D. Adams, Y. Zhu, G. Chen, X. Liu, J. Wei, I. Chiorescu, et al., arXiv preprint arXiv:1507.07978 (2015).
[19] Y.-Y. Wang, Q.-H. Yu, and T.-L. Xia, arXiv preprint arXiv:1603.09117 (2016).
[20] S. Borisenko, arXiv preprint arXiv:1507.04847 (2016).
[21] S.-Y. Xu, I. Belopolski, N. Alidoust, M. Neupane, G. Bian, C. Zhang, R. Sankar, G. Chang, Z. Yuan, C.-C. Lee, et al., Science **349**, 613 (2015).
[22] B. Lv, H. Weng, B. Fu, X. Wang, H. Miao, J. Ma, P. Richard, X. Huang, L. Zhao, G. Chen, et al., Phys. Rev. X **5**, 031013 (2015).
[23] S.-Y. Xu, N. Alidoust, I. Belopolski, Z. Yuan, G. Bian, T.-R. Chang, H. Zheng, V. N. Strocov, D. S. Sanchez, G. Chang, et al., Nature Physics (2015).
[24] I. Belopolski, S.-Y. Xu, D. Sanchez, G. Chang, C. Guo, M. Neupane, H. Zheng, C.-C. Lee, S.-M. Huang, G. Bian, et al., arXiv preprint arXiv:1509.07465 (2015).
[25] L. Yang, Z. Liu, Y. Sun, H. Peng, H. Yang, T. Zhang, B. Zhou, Y. Zhang, Y. Guo, M. Rahn, et al., Nature physics **11**, 728 (2015).
[26] S.-Y. Xu, I. Belopolski, D. S. Sanchez, C. Zhang, G. Chang, C. Guo, G. Bian, Z. Yuan, H. Lu, T.-R. Chang, et al., Science advances **1**, e1501092 (2015).
[27] N. Xu, H. Weng, B. Lv, C. Matt, J. Park, F. Bisti, V. Strocov, E. Pomjakushina, K. Conder, N. Plumb, et al., Nature communications **7**, 11006 (2016).
[28] H. B. Nielsen and M. Ninomiya, Phys. Lett. B **130**, 389 (1983).
[29] V. Aji, Phys. Rev. B **85**, 241101 (2012).
[30] D. T. Son and B. Z. Spivak, Phys. Rev. B **88**, 104412 (2013).
[31] A. Burkov, Phys. Rev. Lett. **113**, 247203 (2014).
[32] E. Gorbar, V. Miransky, and I. Shovkovy, Phys. Rev. B **89**, 085126 (2014).
[33] H.-Z. Lu, S.-B. Zhang, and S.-Q. Shen, Phys. Rev. B **92**, 045203 (2015).
[34] A. Burkov, Phys. Rev. B **91**, 245157 (2015).
[35] J. Xiong, S. K. Kushwaha, T. Liang, J. W. Krizan, M. Hirschberger, W. Wang, R. Cava, and N. Ong, Science **350**, 413 (2015).
[36] C.-Z. Li, L.-X. Wang, H. Liu, J. Wang, Z.-M. Liao, and D.-P. Yu, Nature communications **6**, 10137 (2015).
[37] C. Zhang, E. Zhang, Y. Liu, Z.-G. Chen, S. Liang, J. Cao, X. Yuan, L. Tang, Q. Li, T. Gu, et al., arXiv preprint arXiv:1504.07698 (2015).
[38] X. Huang, L. Zhao, Y. Long, P. Wang, D. Chen, Z. Yang, H. Liang, M. Xue, H. Weng, Z. Fang, et al., Physical Review X **5**, 031023 (2015).
[39] C. Zhang, S.-Y. Xu, I. Belopolski, Z. Yuan, Z. Lin, B. Tong, N. Alidoust, C.-C. Lee, S.-M. Huang, H. Lin, et al., Preprint at http://arxiv. org/abs/1503.02630 (2015).
[40] X. Yang, Y. Liu, Z. Wang, Y. Zheng, and Z.-a. Xu, arXiv preprint arXiv:1506.03190 (2015).
[41] H. Li, H. He, H.-Z. Lu, H. Zhang, H. Liu, R. Ma, Z. Fan, S.-Q. Shen, and J. Wang, Nature communications **7**, 10301 (2016).
[42] F. Arnold, C. Shekhar, S.-C. Wu, Y. Sun, R. D. dos Reis, N. Kumar, M. Naumann, M. O. Ajeesh, M. Schmidt, A. G. Grushin, et al., Nature communications **7**, 11615 (2016).
[43] C.-L. Zhang, S.-Y. Xu, I. Belopolski, Z. Yuan, Z. Lin, B. Tong, G. Bian, N. Alidoust, C.-C. Lee, S.-M. Huang, et al., Nature communications **7**, 10735 (2016).
[44] R. dos Reis, M. Ajeesh, N. Kumar, F. Arnold, C. Shekhar, M. Naumann, M. Schmidt, M. Nicklas, and E. Hassinger, New Journal of Physics **18**, 085006 (2016).
[45] C. Bai, Y. Yang, and K.-W. Wei, Physics Letters A **380**, 764 (2016).
[46] C. Bai, Y. Yang, and K. Chang, Scientific reports **6** (2016).
[47] W.-L. You, X.-F. Wang, A. M. Oleś, and J.-J. Zhou, Applied Physics Letters **108**, 163105 (2016).
[48] C. Yesilyurt, S. G. Tan, G. Liang, and M. Jalil, arXiv preprint arXiv:1605.09108 (2016).
[49] Z. B. Siu, C. Yesilyurt, M. Jalil, and S. G. Tan, arXiv preprint arXiv:1606.08735 (2016).
[50] Y. Chen, J.-H. Chu, J. Analytis, Z. Liu, K. Igarashi, H.-H. Kuo, X. Qi, S.-K. Mo, R. Moore, D. Lu, et al., Science **329**, 659 (2010).
[51] J. Zhang, C.-Z. Chang, P. Tang, Z. Zhang, X. Feng, K. Li, L.-l. Wang, X. Chen, C. Liu, W. Duan, et al., Science **339**, 1582 (2013).
[52] D. Kurebayashi and K. Nomura, Journal of the Physical Society of Japan **83**, 063709 (2014).
[53] T. Sato, K. Segawa, K. Kosaka, S. Souma, K. Nakayama, K. Eto, T. Minami, Y. Ando, and T. Takahashi, Nature Physics **7**, 840 (2011).
[54] H. Jin, J. Im, and A. J. Freeman, Physical Review B **84**, 134408 (2011).

[55] R. Yu, W. Zhang, H.-J. Zhang, S.-C. Zhang, X. Dai, and Z. Fang, Science **329**, 61 (2010).
[56] H. Zhang, C.-X. Liu, X.-L. Qi, X. Dai, Z. Fang, and S.-C. Zhang, Nature physics **5**, 438 (2009).
[57] C.-X. Liu, X.-L. Qi, H. Zhang, X. Dai, Z. Fang, and S.-C. Zhang, Physical Review B **82**, 045122 (2010).